



## Research Article

# PAPR reduction of GFDM signals using moving average filtering scheme for future wireless communications

R. Anil KUMAR<sup>1</sup>, Srinivas THIRUMALA<sup>2,\*</sup>, Tota SREENIVAS<sup>3</sup>, Sarala PATCHALA<sup>4</sup>,  
Srujana GOLLAPALLI<sup>2</sup>

<sup>1</sup>Department of Electronics and Communication Engineering, Aditya College of Engineering and Technology Surampalem, 533437, India

<sup>2</sup>Department of Electronics and Communication Engineering, GIET Engineering College, Rajamahendravaram 533296, India.

<sup>3</sup>Department of Electronics and Communication Engineering, Sri Vasavi Engineering College, Tadepalligudem, 534101, India

<sup>4</sup>Department of Electronics and Communication Engineering, KKR & KSR Institute of Technology and Sciences, Vinjanampadu, 522017, India

## ARTICLE INFO

### Article history

Received: 15 May 2024

Revised: 08 July 2024

Accepted: 24 September 2024

### Keywords:

5G; GFDM; OFDM; MAF;  
Spectral Efficiency; Symbol  
Error Rate

## ABSTRACT

Generalized Frequency Division Multiplexing (GFDM) is a new method for transmitting data in blocks. It is being considered for 5G because it offers better spectral efficiency, lower latency, and more scalability than Orthogonal Frequency Division Multiplexing (OFDM). However, GFDM still faces a problem with high Peak-to-Average Power Ratio (PAPR), which can reduce the system's performance. Therefore, we proposed Moving Average Filtering (MAF) scheme to reduce the high PAPR of the GFDM signals. LAMF operates by taking an average number of GFDM-modulated signal sample points to produce the smoothed output sample points. The computed smoothed values reduce the random high peak noise samples that depend on the length of the filter. In this article, we presented the mathematical analysis of the PAPR of the GFDM signal and the design of a linear average moving filter. The proposed scheme's PAPR and symbol error rate (SER) is compared with different filter lengths and traditional techniques. The proposed scheme's PAPR and Symbol Error Rate (SER) are compared with different filter lengths and traditional techniques. Our findings demonstrate that the PAPR of the MAF\_GFDM signal is reduced to 3.22 dB at CCDF =  $10^{-3}$  with a filter length  $L=64$ , while the symbol error rate is improved to  $0.5 \times 10^{-4}$ . Additionally, the minimum mean square error estimation method is identified as the best estimator, achieving a very low symbol error rate (0.001) at a signal-to-noise ratio of 11 dB. These simulation results obtained using MATLAB demonstrate the effectiveness of the proposed scheme in significantly reducing PAPR and improving SER.

**Cite this article as:** Kumar RA, Thirumala S, Sreenivas T, Patchala S, Gollapalli S. PAPR reduction of GFDM signals using moving average filtering scheme for future wireless communications. Sigma J Eng Nat Sci 2025;43(3):726–736.

### \*Corresponding author.

\*E-mail address: [thirumala.gec@giet.ac.in](mailto:thirumala.gec@giet.ac.in)

This paper was recommended for publication in revised form by  
Editor-in-Chief Ahmet Selim Dalkilic



## INTRODUCTION

Generalized frequency division multiplexing is a recently proposed 5G candidate waveform for future wireless communications. Like OFDM, GFDM is also suffering from high PAPR. It increases the energy and cost efficiency of the hardware equipment. It is a key performance metric of the multicarrier modulation techniques and increases with the number of subcarriers. Due to high PAPR, the linear characteristic of the power amplifier is transformed into the non-linear region that creates the in-band and out-of-band interference of the received signal. Therefore, the symbol error rate increases, which degrades the GFDM system performance. It is especially a significant concern in the uplink scenario, which increases the radiation power of the user equipment (UE) which reduces the system's lifetime. GFDM with a reduced peak-to-average power ratio (PAPR) has several potential uses in 5G networks. These include enhanced mobile broadband, massive machine-type communications, satellite communications, and ultra-reliable low-latency communications.

To address the PAPR issue in 4G, Ghosh et al. proposed a single carrier orthogonal frequency division multiplexing (SC-OFDM) modulation scheme for the uplink scenario [1]. Meanwhile, Tao Jiang et al. introduced a multi-block tone reservation (MBTR) method to reduce PAPR in OQAM-OFDM [2]. The basic idea is to generate the reverse peak canceling signal with the help of a weighted least-square algorithm to remove the high peaks of the OFDM signal effectively. This method offers a low PAPR with less computational complexity than tone reservation. Kelvin Anoh et al. identified a problem in interactive clipping and filtering (ICF): the method requires more iteration to achieve the desired PAPR. It increases the processing time and system power. Hence, the proposed optimized ICF reduces the number of iterations using a second-order cone program [3],[4].

### Literature Survey

Several methods have been proposed and implemented over the years to tackle the problem of high PAPR in multicarrier transmission systems. These methods are explained in following section.

MinhoeKim et al. recently designed [5] a novel encoder architecture using deep learning for PAPR reduction. The function of the network is mapping and de-mapping of constellation symbols on each sub-carrier is done adaptively with a deep learning algorithm. This technique is jointly minimized both the PAPR and BER of the OFDM system. On the other hand, Michailow et al. addressed drawbacks of GFDM similar to other multicarrier signals, that the significant PAPR signals can quickly saturate the transmit power amplifier and cause degradation in BER performance and out-of-band emissions [6]. Therefore, Michailow et al. proposed a WHT-GFDM scheme to reduce the high PAPR and achieve low OOB emission and good BER performance [7].

Zahra Sharifian et al. [7] proposed a linear, data-independent precoder to reduce the variance of instantaneous power (IP) without increasing out-of-band (OOB) radiation or degrading the bit error rate. Based on this approach, a GFDM system with  $M = 5$ ,  $N = 256$ ,  $P = 4$ , and localized frequency division multiple access (LF-DMA) is considered in their study. Compared with the DFT precoder, the proposed method provides a lower PAPR [8]. It is due to the result of the optimization of the precoding matrix. Also discussed existing methods such as signal clipping and filtering, exponential, polynomials-based companding techniques [9],[10],[11]. Hassan et al. [12] proposed a low-complexity linear average moving filtering scheme for PAPR reduction and symbol error rate of OFDM signals with different filter lengths.

Liu et al. did [13] a theoretical analysis of PAPR for critically and over-sampled GFDM signals and derived exact closed-form expressions. The problem of high PAPR in any multicarrier system occurs due to the superposition of modulated subcarriers of random data. According to the properties of the GFDM block structure, there is no interference between adjacent signal blocks when compared with OFDM. Hyunmyung et al. [14] research article discussed the importance of the orthogonality of subcarriers and synchronization to reduce the system the latency for 5G. Recently proposed GFDM is the best solution for the above requirements to reduce the latency. However, the superposition of multiple sub-symbols and subcarriers results in high PAPR. Author proposed a selective level mapping (SLM) technique to reduce the high PAPR and out-of-band interference in GFDM signals [15], [16]. SLM is not a signal distortion technique and does not require extra side information. The basic idea of this technique is selecting the low peak values from generated GFDM data sequence.

Yaqin Zhao et al. [17] addressed computational complexity and severe signal distortion with increasing subcarriers and observed that signal recovery is not possible by clipping technique. To reduce the PAPR, proposed a new majorizing companding technique (MCT) scheme in the GFDM system. This method reduces the high peak signals and expands low peak signals up to the threshold level (average value). Thus, peak power decreases, and average power increases. Therefore, the PAPR of the GFDM signal is reduced.

The above techniques are non-linear techniques that cause significant in-band and out-of-band distortions and degrade the system's spectral efficiency and symbol error rate performance. Previous literature studies have not considered any filtering techniques, but Andres Ortega [18] considered filtering techniques along with clipping to improve the out-band emission but not the effective recovery of the GFDM signals at the receiver. Therefore, this paper proposed a novel Moving Average Filter to reduce the PAPR and out band emission of the GFDM system, referred to as the MAF-GFDM system.

The following are the key benefits of MAF scheme PAPR reduction in GFDM signals:

- The loss of orthogonality between subcarriers in the OFDM system degrades the Symbol Error Rate but GFDM is a non-orthogonal multicarrier modulation technique. Therefore, we proposed a moving average filter for the GFDM system because it does not distort orthogonality among subcarriers at the receiver.
- The low pass filter features of the moving average filter effectively suppress the out-of-band emissions that result in improved symbol error rate and spectral efficiency.
- The MAF reduces transmitted power and signal distortion, thus eliminating the need for high power amplification at the transmitter. This results in less power consumption and enhances the energy efficiency of the system

This scheme also improves the significant symbol error rate performance of the system. The main advantages of this technique are described as follows:

- This proposed scheme is simple to implement for any number of subcarriers and does not require any extra side information to reduce the PAPR.
- The low pass filter features of the moving average filter effectively suppress the out-of-band emissions that result in improved symbol error rate and spectral efficiency.
- Minimum mean square error and zero-forcing detection schemes are implemented to recover the original data symbols, which also help to compensate for the frequency of selective fading and filtering.

The paper is planned with the following sections: Introduction to the topic, literature review, and objectives are explained in section 1. Section 2 discussed the modulation and demodulation of GFDM and derived mathematical expressions for PAPR. Section 3 proposed MAF\_GFDM and section 4 addressed the performance of PAPR, SER,

and different detection techniques. Finally, conclusions are drawn in section 5.

### System Model

GFDM is a flexible, non-orthogonal, block-based, filter bank innovative multicarrier modulation method for 5G new radio. In this method, subcarriers and transmission filters provide circular shifting in frequency and time, respectively. The proposed GFDM transceiver elements are shown in Figure 1.

At the transmitter section, the binary data is input to the mapper, it converts bits into QPSK constellation symbols and then these symbols are multicarrier modulated with a GFDM modulator (A). Next, the proposed moving average filter reduces the signal's high peaks, and then the signal is up-converted. The Cyclic Prefix is added to the signal before transmission into radio channels to avoid inter-symbol interference. Due to the multipath environment signal is faded and received by the antenna. In the receiver section, a low noise amplifier boosts the GFDM received signal and maintains the receiver's sensitivity above the sufficient noise floor. The cyclic prefix of the received signal is removed, and GFDM is demodulated. Finally, a de-mapper decodes original bits from symbols[19].

### GFDM Modulation and Demodulation

The design of the GFDM modulator block plays an important role. The modulator contains  $N=M.K$  input data symbols. In which,  $M$  sub-symbols are carried by  $K$  number of subcarriers. Therefore, the matrix representation of data symbols  $\vec{d}_m$  for  $K$  subcarriers is as shown in equation (1).

$$\vec{d}_m = [d_{0,m}, \dots, d_{K-1,m}]^T \quad (1)$$

To perform the pulse shaping on generated symbols and each set of symbols is up sampled by factor  $N$  as follows.

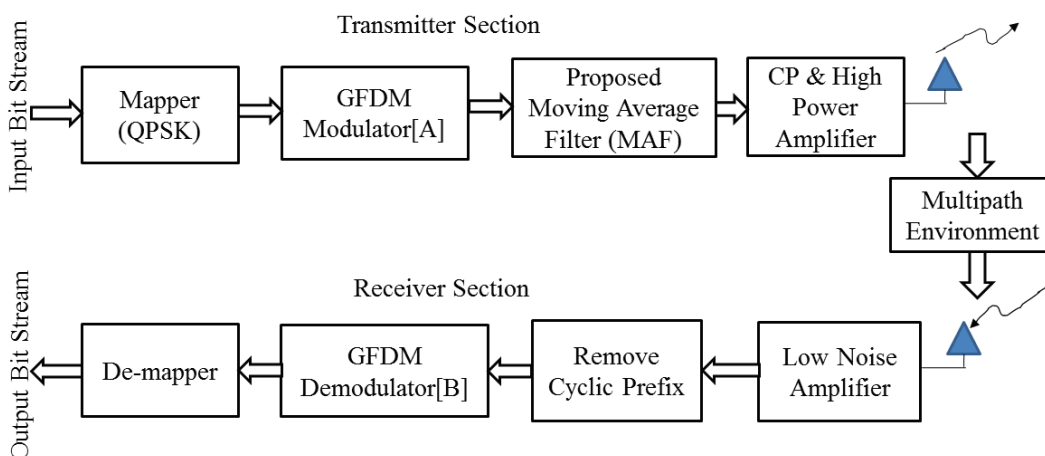


Figure 1. Proposed MAF-GFDM transceiver.

$$g_{k,m}[n] = g[(n - mK) \bmod N]. e^{\frac{-2\pi kn}{K}} \quad (2)$$

Where,  $m$  is sub-symbol index with length  $m = 0, 1, 2, \dots, M - 1$

$k$  is sub-carrier index with length  $k = 0, 1, 2, \dots, K - 1$

$n$  is index of the sampling time with length  $n = 0, 1, 2, \dots, N - 1$

$g[n]$  is transmit prototype filter of  $g_{k,m}[n]$  with frequency and time shifted versions.

Modulo operation is to perform the circularly time shift of  $g_{k,m}[n]$

Finally,  $e^{j2\pi kn/K}$  is complex exponential term perform the frequency shift.

To perform the simulation operations and standard demodulation methods at the receiver, equation (2) is represented in matrix form

$$x = Ad \quad (3)$$

Where,  $d$  and  $x$  are representations of input and output data vectors respectively.  $A$  is the GFDM modulation matrix with dimensions  $MK \times MK$  as shown in equation (4). The special characteristic of the matrix is that it satisfies the frequency and time-shifting properties. The elements of matrix is impulse responses of transmit filter  $g_{k,m}[n]$ . This scheme generates the resource elements as block wise and then transmitted it through the antenna system.

$$A = \begin{bmatrix} g_{0,0}[0] & \dots & g_{K-1,0}[0] & \dots & g_{0,M-1}[0] & \dots & g_{K-1,M-1}[0] \\ g_{0,0}[1] & \dots & g_{K-1,0}[1] & \dots & g_{0,M-1}[1] & \dots & g_{K-1,M-1}[1] \\ \dots & \dots & \dots & \dots & \dots & \dots & \dots \\ g_{0,0}[N-1] & \dots & g_{K-1,0}[N-1] & \dots & g_{0,M-1}[N-1] & \dots & g_{K-1,M-1}[N-1] \end{bmatrix}_{MK \times MK} \quad (4)$$

The 3-D view of the modulation matrix with time and frequency indices is shown in Figure 2. There are repeated patterns of the magnitude of elements of matrix

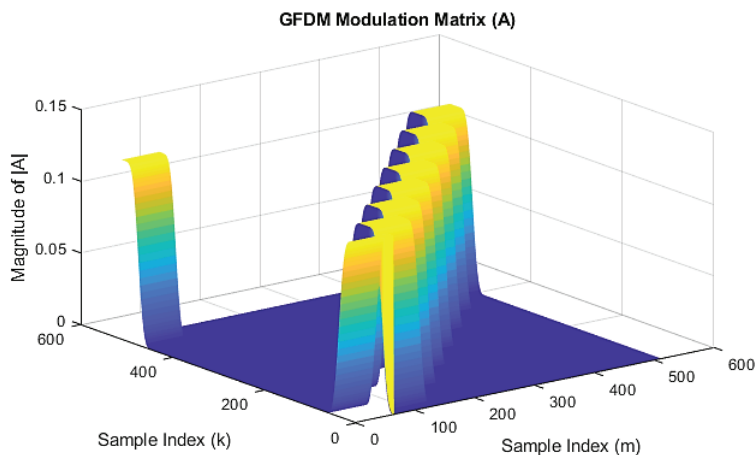


Figure 2. The characteristics of GFDM modulation matrix.

A. It contains the responses of the pulse-shaping filter for all possible time and frequency shifts. It results in a block-based diagonal structure. It results in a block based diagonal structure.

**Matched filter detection**

Matched filters are used at the receiver to maximize the SNR in the presence of additive noise. In MIMO-GFDM, the root-raised cosine filter works as a Nyquist filter and doesn't allow the ISI (Inter symbol Interference) at the output of the GFDM demodulator  $B$  satisfies the following expression (5). Here,  $A^H$  is the Hermitian of the GFDM modulation matrix.

$$B_{MF} = A^H \quad (5)$$

However, due to the non-orthogonality of GFDM while pulse shaping processing, it carry some self-interference that cannot be eliminated using a matched filter.

**Zero forcing detection**

Zero forcing detection is a method to restore the signal after the channel equalizer by applying inverse frequency response to the received signal ( $Y$ ). This method not only enhances the SNR and also eliminates the self-interference at the receiver. First, pre-multiply  $Y$  with  $H^H$  then Equation (6) possessed through channel equalizer, then the resultant output signal  $Z$  is

$$Z = H^H Y \quad (6)$$

$$Z = H^H HX + H^H W \quad (7)$$

Here,  $R = H^H H$  is a square matrix with order  $RXT$ . The best solution for MIMO-GFDM is Zero forcing detection in which  $Z$  is pre-multiplied by  $R^{-1}$ .

$$\hat{X} = X + R^{-1}HW \tag{8}$$

The original GFDM symbols are demodulated when noise is minimized. In the presence of noise, distortion, interference and due to bit synchronization and the data streams are altered and received wrongly.

**MMSE detection**

The linear mean square error receiver had an interchange between noise enhancement and self-interference and is defined as

$$C_{MMSE} = (R_w^2 + A^H H^H H A)^{-1} \tag{9}$$

The term  $A^H H^H$  represents the trade-off between noise enhancement and self-interference. The term  $R^2 \omega$  denotes the covariance matrix of noise. Finally, the demodulated signal is de-mapped, decoded and make progress of recovered binary data.

**Mathematical Analysis of Papr in GFDM and OFDM Systems**

GFDM is suffering from PAPR problems, resulting in the degradation of the communication system. The PAPR value of the GFDM transmitted signal is high as compared to OFDM. The generated GFDM signal shown in Figure 3 with system parameters  $K=4$  and  $M=4$ . The mathematical expression of PAPR of GFDM and OFDM signals is derived in [10]. PAPR of the signal is defined as which is the ratio between the peak power of the signal to the average power

$$PAPR = \frac{\text{Peak Power}}{\text{Average Power}} = \frac{\text{Max}_{0 \leq n \leq N-1} [|x[n]|^2]}{E[|x[n]|^2]} \tag{10}$$

Here,  $E[\bullet]$  is an expectation operator and  $x(n)$  is a GFDM modulated signal as shown in equation (11).

$$x[n] = \sum_{m=0}^{M-1} s_m[n] \cdot g[(n-mK) \bmod N] \tag{11}$$

Where, new signal  $s_m[n]$  is carry the data symbols on subcarriers

$$s_m[n] = \sum_{k=0}^{K-1} d_{k,m}[n] \cdot e^{-\frac{2\pi kn}{K}} \tag{12}$$

The equation (12) separates baseband data symbols that are modulated with different subcarriers without filtering. Here, sub-symbols are independent identically distributed (IID) random data. According to the central limit theorem, for the large number of subcarriers the  $s_m[n]$  can be modelled as a Complex Circular Symmetric Gaussian Random Variable (CCSGR).

$$s_m[n] = CGN(0, K \sigma_d^2) \tag{13}$$

Here,  $CGN(\bullet, \bullet)$  represents the Complex Gaussian Distribution and  $\sigma_d^2$  is the variance of the data symbol  $d_{k,m}$ . Linear sum of the large number of Gaussian random variables is also a Gaussian random variable. Clearly, the sampled signal  $x(n)$  is a non-stationary random signal. It exhibits a Gaussian Stochastic random process

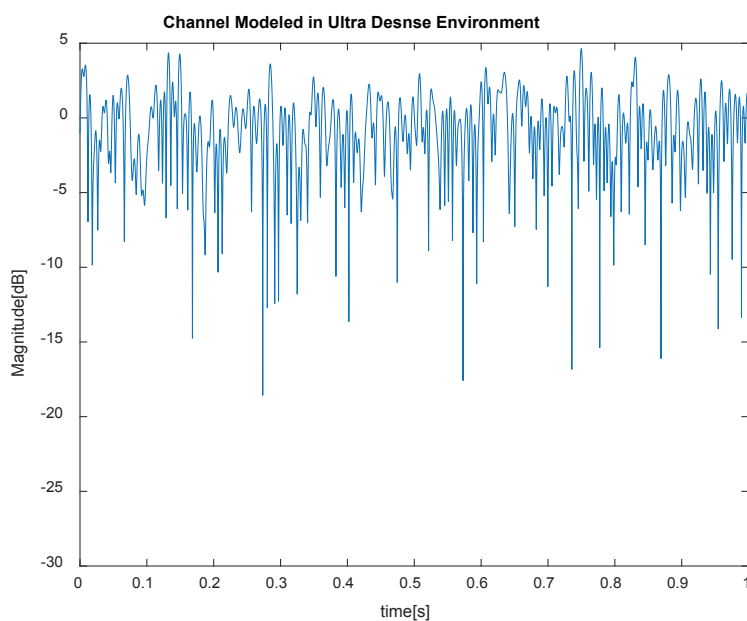


**Figure 3.** GFDM modulated signal with low and high peaks.

with different variances. If the sum term in equation (13) changes at different sample indices  $n$  with certain pulse shaping filters, the amplitude of a complex Gaussian random variable follows a Rayleigh distribution. Therefore, the Cumulative Distribution Function (CDF) of the Rayleigh distribution for  $x[n]$  is given by the following expression.

$$P_{cdf}(x) = \text{Prob}\{|x(n)| \leq x\} = 1 - e^{-\frac{x^2}{\sigma_n^2}} \quad (14)$$

We can easily derive the Complementary CDF (CCDF) of PAPR for GFDM signals by just replacing  $\varepsilon^2$  with the targeted PAPR threshold value  $\delta$  in equation (15).

$$P_{cdf}(\delta) = \text{Prob}\{PAPR_{GFDM} > \delta\} \quad (15)$$

The formula for the CCDF of PAPR of a GFDM modulated signal under the critical sampling hypothesis is shown in equation (15). Here, PAPR is calculated for discrete time signal  $x(n)$ , but in the case of practical continuous time signal  $x(t)$  after analog to digital conversion, which may have high PAPR because discrete time signal does not include all the peaks of  $x(t)$ . Therefore, loss of accuracy for continuous time signals.

Furthermore, we can extend the formula  $P_{ccdf, GFDM}(\delta)$  for calculations of PAPR in OFDM signals. As we discussed OFDM modulation scheme, we can derive from GFDM by setting subsymbols value  $M=1$ . Hence, the prototype filter performs the operation of a rectangular filter. Therefore, there is no operation of circular time shifting and the principle of superposition with pulse shaping filters. The filter coefficients of rectangular pulse are represented with normalized total power.

$$g_{k,m}[n] = \begin{cases} \frac{1}{\sqrt{K}} & n = 0, 1, 2, \dots, K - 1 \\ 0 & K, K + 1, \dots, KM - 1 \end{cases} \quad (16)$$

The filter equation (16) is introduced in GFDM signals, and the equation (17) is deduced to

$$\therefore P_{ccdf, GFDM}(\delta) = 1 - (1 - e^{-\delta})^{KM} \quad (17)$$

When  $M=1$  the equation turns into CCDF of PAPR of OFDM signal

$$\therefore P_{ccdf, OFDM}(\delta) = 1 - (1 - e^{-\delta})^K \quad (18)$$

Whenever,  $M=1$  (OFDM), symbols are modulated  $K$  number of subcarriers that leads to high PAPR in the OFDM system. Equation (18) is the well-known CCDF expression of PAPR for OFDM signals only depends on the number of subcarriers used for IFFT operation. As stated before, if the number of subcarriers increases, then PAPR

increases exponentially in the OFDM system. If  $M>1$ , then the GFDM modulation scheme is increases the PAPR. Because the number of sub-symbols ( $M$ ) in each of the  $K$  subcarriers. But, the pulse shape applied in the GFDM system gives control over every peak and the average value of the transmitted signal. The high PAPR value does not affect the orthogonality of the transmitted signal but is based on the PAPR reduction technique, which results in more bit errors. Hence any multicarrier modulation techniques take the complex design of the receiver.

### PROPOSED MAF\_GFDM SYSTEM

The moving average filter is a linear time-invariant, easily implemented, most useful, optimal digital filter for signal processing applications to remove the noise and interferences of slowly varying signals [20], [21]. The name implies that it operates by taking the average number of sample points of GFDM modulated signal to produce the smoothed output sample points. The mathematical representation of finite impulse response is as shown in equation (19). Here,  $L$  is the length of the filter sequence.

$$h[n] = \begin{cases} \frac{1}{L} & 0 \leq n \leq L - 1 \\ 0 & \text{Otherwise} \end{cases} \quad (19)$$

The output of the moving average filter is the convolution of GFDM signal  $x[n]$  and the impulse response of the filter and performs the smoothing on the GFDM signal.

$$y[n] = h[n] * x[n] = \sum_{l=0}^{L-1} h[l] x[n-l] \\ = \frac{1}{L} \left[ x[n] + \underbrace{x[n-1] + \dots + x[n-L+1]}_{\text{Inter-carrier interference}} \right] \quad (20)$$

The filtering equation contains the original signal and interferences from other subcarriers, resulting in Inter-Carrier-Interference (ICI). It causes orthogonality between subcarriers of the OFDM system that degrade the Symbol Error Rate. GFDM is a non-orthogonal multicarrier modulation technique. Therefore, we proposed a moving average filter for the GFDM system because it does not distort orthogonality among subcarriers at the receiver.

$$H(\omega) = \frac{1}{L} \sum_{l=0}^{L-1} e^{-j\omega l} = D_L(\omega) \cdot e^{-j\omega(L-1)/2} \quad (21)$$

The term  $D_L(\omega)$  is a Dirichlet function defined in [22] and calculated as follows

$$D_L(\omega) = \frac{1}{L} \cdot \frac{\sin(\frac{\omega L}{2})}{(\frac{\omega}{2})} \quad (22)$$

Equation (21) represents the low pass and linear phase characteristics. The major lobe of the magnitude response is not exactly rectangular and has some side lobes. For an FIR filters, the width of the major lobe is inversely proportional to the filter length. Higher  $L$  values lead to reduced side lobes that improve the low-pass filter's smoothing performance.

Suppose the moving average filter receives the over-sampled GFDM symbols such as  $h = [h(0), h(1), h(2), \dots, h(L-1)]^T$  with range  $1 \leq n \leq M$ . Therefore, the output for  $k^{\text{th}}$  symbol block of the filter is represented as equation (23), [23,24].

$$\hat{y}_M(k) = H_M(h) x_M(k) + \tilde{H}_M(h) x_M(k-1) \quad (23)$$

Here,  $H_M(h)$ ,  $\tilde{H}_M(h)$ , are lower and upper triangular  $MXM$  matrices and also referred to as Toeplitz filtering coefficients. Equation (23) depends on both the present symbol  $X_M[k]$  and past symbol  $X_M[k-1]$ . This will happen due to the moving average filter memory that creates the Inter Block Interference (IBI) between successive blocks of the GFDM symbols. To avoid the IBI, the data blocks must be transmitted and received independently. Consequently, it is assumed that all inputs in front of  $X_{M,k}(0)$  are zeros as well as input data symbols after  $X_{M,k}(M-1)$  are zeros. Hence, we can rewrite the mathematical expression for  $k^{\text{th}}$  the output symbol block with avoided Inter Block Interference as follows:

$$y_M(k) = [y_{M,k}[0], \dots, y_{M,k}[M-1]]^T = H_M[h] x_M[k] \quad (24)$$

Where, first received GFDM symbol  $y_{M,k}[0] = \frac{x_{M,k}[0]}{L}$ ,

Second received GFDM symbol  $y_{M,k}[1] = \frac{[x_{M,k}[0] + x_{M,k}[1]]}{L}$ ,

Similarly for  $M^{\text{th}}$  GFDM symbol

$$y_{M,k}[M-1] = \frac{[x_{M,k}[M-L] + x_{M,k}[M-1]]}{L} \quad (25)$$

Therefore, the significant advantage of the moving average filter is easy implementation due to its recursive nature of the filter. The recursive filter expression is shown in the following equation (26). It is also observed; equation (24) needed more multiplications, additions, and subtractions than equation (26).

$$y_{M,i}[n] = y_{M,i}[n-1] + \frac{1}{L} [x_{M,i}[n] - x_{M,i}[n-L]] \quad (26)$$

#### Average Transmitted Power of MAF\_GFDM signal

Trace of the matrix is defined as the sum of the diagonal elements of the received signal matrix. The application of the trace is to find the average power in random GFDM signal as shown in equation (27).

$$E[\|y_N[k]\|^2] = E[y_N[k] y_N^H[k]] = \frac{\text{tr}(E\{y_N[k] y_N^H[k]\})}{N} \quad (27)$$

Substitute equation (24) in (27)

$$E[\|y_N[k]\|^2] = \frac{\text{tr}(E\{H_M(h) x_N[k] x_N^H[k] H_M^H(h)\})}{N} \quad (28)$$

Where,  $E\{x_N[k] x_N^H[k]\} = \sigma_s^2$  is MAF\_GFDM signal power.

$$E[\|y_N[i]\|^2] = \sigma_s^2 \frac{\text{tr}(E\{H_M(h) H_M^H(h)\})}{N} \quad (29)$$

Equation (29) represents the sum of diagonal filter coefficients (Trace of the matrix) that results in the following equation form.

$$\therefore \text{Average power} = \sigma_s^2 \cdot \left[ \frac{\left( \frac{1+2+\dots+L}{L^2} \right) + \left( \frac{M-L}{L} \right)}{M} \right] \quad (30)$$

Finally, the summation of arithmetic numbers implies the following result:

$$\frac{E[\|y_M[k]\|^2]}{M} = \sigma_s^2 \left[ \frac{2M-L+1}{2ML} \right] \quad (31)$$

## PERFORMANCE ANALYSIS

Simulation results are obtained for this section's proposed scheme on the MAT lab working platform. GFDM modulated signal is generated by considering  $K=128$  and  $M=5$  in an ultra-dense multipath environment with path loss exponent  $n=5$  and then the signal is processed through a moving average filter. Performance of PAPR and BER results are obtained for OFDM signal and different filter lengths  $L$ .

The complementary cumulative distribution function is a crucial statistical tool. It is used to evaluate the effectiveness of peak-to-average power ratio reduction techniques in wireless communication systems. It is particularly used in multicarrier modulation techniques such as OFDM, GFDM, FBMC and UFMC. The CCDF is used to describe the probability that the PAPR of a transmitted signal exceeds a certain threshold. Mathematically represented as  $\Pr(\text{PAPR} > \delta)$ . Here  $\delta$  is threshold PAPR value. This function provides a statistical measure of how often the signal peaks exceed a specified level.

Figure 4 shows the CCDF of peak to average power ratio of GFDM and OFDM signals with different filter lengths. Input data samples are random which results in random

**Table 1.** Simulation parameters

System Parameter	Notation	Significant Value
Number of Subcarriers	$K$	128
Number of Subcarriers	$M$	5
Modulator	$A$	GFDM
Demodulator	$B$	Inverse GFDM
Moving Average filter lengths	$L$	2,8,64
Demodulation technique	ZF	Zero Forcing (ZF) Receiver
Pulse Shaping Filter	$g$	RRC filter
Roll of factor	$\alpha$	0.5
Length of Cyclic Prefix (CP)	CP	7% of GFDM Symbol
Path loss Exponent Value	$n$	5
Doppler Frequency	$f_d$	50Hz

PAPR values. Therefore, these statistical PAPR values are calculated using the function of CCDF. From equation (17) and (18) it is observed that the PAPR of the GFDM signal is high then compared to existing OFDM. If the number of subsymbols and subcarriers increases in MAF\_GFDM scheme it will result in high PAPR. Therefore, the PAPR of GFDM is 6.82 dB at  $CCDF=10^{-3}$ .

PAPR values are calculated at  $CCDF=10^{-3}$  and it is observed PAPR value is diminishing from without filtering process to with average moving filtering scheme for different filter lengths. Reason for this from equation (30) or equivalent equation (31) if the filter length increases, then the average transmitted power is decreased. Furthermore,

the characteristic of the low pass filter is linear. The major lobe of the magnitude response is not exactly rectangular and has some side lobes. For an FIR filters, the width of the major lobe is inversely proportional to the filter length. The higher values of  $L$  is leads to reduce the side lobes. It results in the improved smoothing performance of the low-pass filter, which removes high peak noise in the GFDM modulated signal. Hence, the PAPR value of the MAF\_GFDM signal is reduced to 3.22dB at  $CCDF=10^{-3}$  with filter length  $L=64$ , as shown in Figure 4.

Figure 5 shows the performance of the symbol error rate of OFDM and GFDM with different filter lengths. The original OFDM and filtered GFDM signals are transmitted

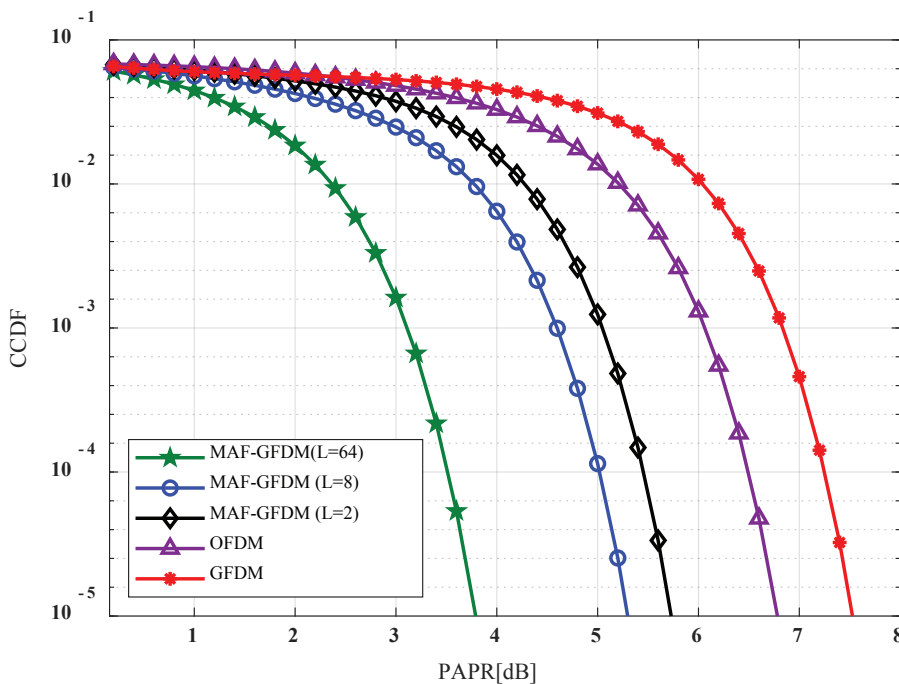


**Figure 4.** PAPR of MAF\_GFDM with different filter lengths.

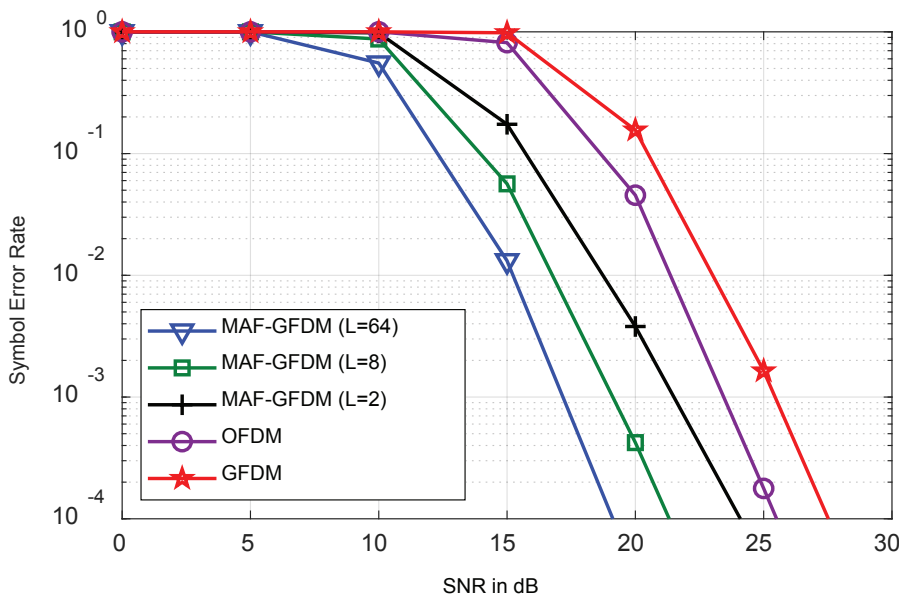


Figure 5. The symbol error rate of MAF\_GFDM system with different lengths.

through three rays dynamic Rayleigh fading channel and are faded at Doppler frequency at 50Hz. While generating GFDM signal, we have initial carrier frequency 900MHz. The receiver assumed that channel state information was perfectly known to the receiver. We have implemented matched filter, zero forcing and minimum mean square estimation techniques to detect the MAF\_GFDM signal. ZF detection scheme not only enhances the SNR and also eliminates the self-interference at the receiver. On the other hand, the MMSE technique improves the SNR in a

multipath path fading environment, which result in less inter carrier interference and minimized symbol errors of the MAF\_GFDM signal. Hence, MMSE is the best detection technique among existing techniques, as shown in Figure 6. It has a very low symbol error rate of 0.001 at the signal to noise ratio 11dB.

Reduction of PAPR yields less transmitted power and distortion of the signal. Therefore, signal cannot be strained to lead by the high-power amplifier at the transmitter. Due to this, there is no significant loss in signal while employing

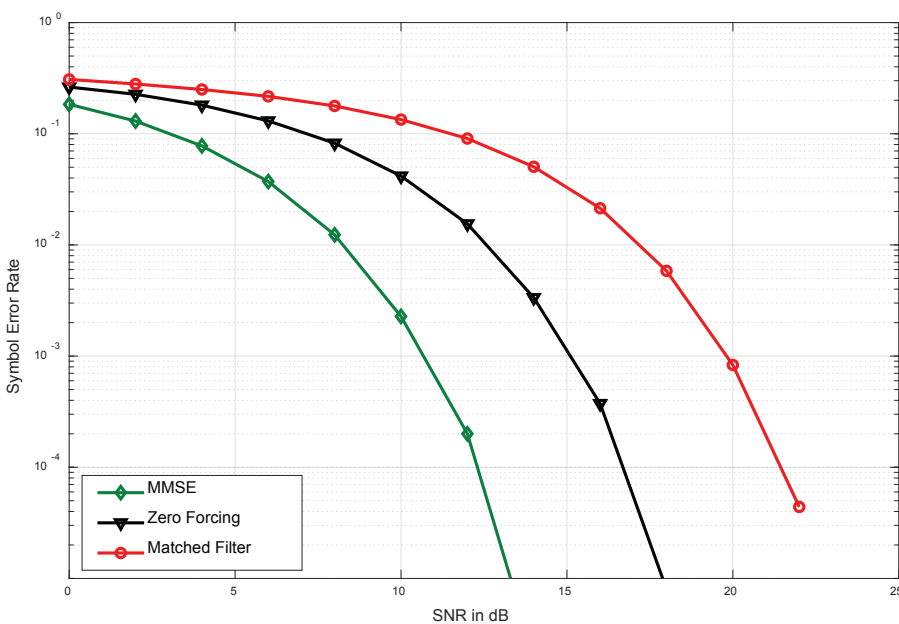


Figure 6. Symbol error rate of MAF\_GFDM signal with different detection techniques.

**Table 2.** Comparisons of PAPR and SER values of MAF\_GFDM system with different filter lengths

System model	Order of the filter	PAPR (dB) value at CCDF = $10^{-3}$	SER @ SNR = 18 dB
GFDM	-----	6.82	$15.60 \times 10^{-2}$
OFDM	-----	6.07	$4.55 \times 10^{-2}$
MAF_GFDM	2	5.05	$3.79 \times 10^{-3}$
	8	4.61	$4.22 \times 10^{-4}$
	64	3.22	$0.5 \times 10^{-4}$

the filtering process before transmission. Therefore, the symbol error rate is improved from the original GFDM to the MAF\_GFDM signal, that we have observed is improved to  $0.5 \times 10^{-4}$  at filter length  $L=64$ .

## CONCLUSION

This research article proposes an efficient, simple moving average filter technique for the PAPR reduction of GFDM signals. The Proposed scheme is employed by taking the average number of GFDM modulated signal sample points to produce the smoothed output sample points. The computed smoothed values reduce the random high peak noise samples that depend on the length of the filter  $L$ . We derived and discussed mathematical expressions for PAPR of the OFDM and GFDM signals as a function of CCDF. From the expressions, we conclude PAPR value is increased with the number of subcarriers and sub-symbols. In our proposed method, higher values of  $L$  leads to reduction side lobes that result in the improved smoothing performance of the low pass filter, which removes high peak noise in GFDM modulated signal. Hence, the PAPR value of the MAF\_GFDM signal is reduced to 3.22dB at CCDF= $10^{-3}$  with filter length  $L=64$ . On the other hand, we have observed symbol error rate is improved to  $0.5 \times 10^{-4}$  at filter length  $L=64$  and also minimum mean square error estimation method is the best estimator due to its very low symbol error rate (0.001) at the signal to noise ratio of 11dB.

## Future Work

Future work should focus on optimizing the MAF scheme to minimize its computational resource requirements, processing time, and power consumption, ensuring that it does not negatively impact system performance and efficiency in real-world 5G applications. Additionally, further research is needed to address the potential trade-offs between PAPR reduction, symbol error rate, and spectral efficiency, with the aim of achieving a balanced solution that maintains ultra-low latency and high performance.

## ACKNOWLEDGEMENTS

This work was supported by the Aditya College of Engineering College(A), Research centre in Electronics

and Communication Engineering. The authors would like to thank for this support.

## AUTHORSHIP CONTRIBUTIONS

Authors equally contributed to this work.

## DATA AVAILABILITY STATEMENT

The authors confirm that the data that supports the findings of this study are available within the article. Raw data that support the finding of this study are available from the corresponding author, upon reasonable request.

## CONFLICT OF INTEREST

The author declared no potential conflicts of interest with respect to the research, authorship, and/or publication of this article.

## ETHICS

There are no ethical issues with the publication of this manuscript.

## REFERENCES

- [1] Ghosh A, Ratasuk R, Xiao W. Method and apparatus for transmission of uplink control signaling and user data in a single carrier orthogonal frequency division multiplexing communication system. Google Patents; 2012 Jul 17.
- [2] Jiang T, Ni C, Ye C, Wu Y, Luo K. A novel multi-block tone reservation scheme for PAPR reduction in OQAM-OFDM systems. IEEE Trans Broadcast 2015;61:717–722. [CrossRef]
- [3] Anoh K, Tanriover C, Adebisi B. On the optimization of iterative clipping and filtering for PAPR reduction in OFDM systems. IEEE Access 2017;5:12004–12013. [CrossRef]
- [4] Merah H, Merah L, Tahkoubit K, Talbi L. Iterative filtering PAPR reduction method for OFDM modulation in fifth-generation cellular networks. Int J Sens Wirel Commun Control 2023;13:385–394. [CrossRef]

- [5] Kim M, Lee W, Cho D. A novel PAPR reduction scheme for OFDM system based on deep learning. *IEEE Commun Lett* 2018;22:510–513. [\[CrossRef\]](#)
- [6] Deepthi PS, Priyanka VS, Anil Kumar R, Kumar S. Review of 5G communications over OFDM and GFDM. In: Kumar A, Mozar S, editors. *ICCCE 2020*. Singapore: Springer; 2021. (Lecture Notes in Electrical Engineering; vol. 698). [\[CrossRef\]](#)
- [7] Michailow N, Mendes L, Matthé M, Gaspar I, Festag A, Fettweis G. Robust WHT-GFDM for the next generation of wireless networks. *IEEE Commun Lett* 2015;19:106–109. [\[CrossRef\]](#)
- [8] Kumar RA, Prasad KS. Performance analysis of an efficient linear constellation precoded generalized frequency division multiplexing with index modulation in 5G heterogeneous wireless network. *Int J Commun Syst* 2021;34:e4732. [\[CrossRef\]](#)
- [9] Sharifian Z, Omid M, Saeedi-Sourck H, Farhang A. Linear precoding for PAPR reduction of GFDM. *IEEE Wirel Commun Lett* 2016;5:520–523. [\[CrossRef\]](#)
- [10] Sendrei L, Marcheviský S, Michailow N, Fettweis G. Iterative receiver for clipped GFDM signals. In: 2014 24th International Conference Radioelektronika. 2014. p. 1–4. [\[CrossRef\]](#)
- [11] Liu K, Deng W, Liu Y. An efficient nonlinear companding transform method for PAPR reduction of GFDM signals. In: 2018 IEEE/CIC International Conference on Communications in China (ICCC). 2018. p. 460–464. [\[CrossRef\]](#)
- [12] Sharifian Z, Omid M, Farhang A, Saeedi-Sourck H. Polynomial-based compressing and iterative expanding for PAPR reduction in GFDM. In: 2015 23rd Iranian Conference on Electrical Engineering. 2015. p. 518–523. [\[CrossRef\]](#)
- [13] Liu K, Deng W, Liu Y. Theoretical analysis of the peak-to-average power ratio and optimal pulse shaping filter design for GFDM systems. *IEEE Trans Signal Process* 2019;67:3455–3470. [\[CrossRef\]](#)
- [14] Oh H, Yang H. PAPR reduction scheme using selective mapping in GFDM. *J Korean Inst Commun Inf Sci* 2016;41:698–706. [\[CrossRef\]](#)
- [15] Rodriguez JT, Colone F, Lombardo P. Supervised reciprocal filter for OFDM radar signal processing. *IEEE Trans Aerosp Electron Syst* 2023;59:3871–3889. [\[CrossRef\]](#)
- [16] Pradeep Kumar SS, Agees Kumar C, Jemila Rose R. An efficient SLM technique based on chaotic biogeography-based optimization algorithm for PAPR reduction in GFDM waveform. *Automatika* 2024;64:93–103. [\[CrossRef\]](#)
- [17] Zhao Y, Wu C, Wu L, Li C. GFDM system PAPR reduction based on MCT method. 2019. p. 923–934. [\[CrossRef\]](#)
- [18] Ortega Ortega A, Fabbri L, Tralli V. Performance evaluation of GFDM over nonlinear channel. *Event2016 International Conference on Information and Communication Technology Convergence, ICTC 2016 - 30 Nov 2016*. [\[CrossRef\]](#)
- [19] Kumar RA, Prasad KS. Performance analysis of GFDM modulation in heterogeneous network for 5G NR. *Wirel Pers Commun* 2020;116: 2299–2319. [\[CrossRef\]](#)
- [20] Smith SW (editor). *Moving average filters*. In: *Digit Signal Process*. Amsterdam: Elsevier; 2003. p. 277–284. [\[CrossRef\]](#)
- [21] Liu J, Xu Z, Zhang, Z, Lu Herbert Ho-Ching. Research on realization of integrated output current sharing control by moving average filter for synchronous generator. *J Electr Eng Technol* 2024;19:341–350. [\[CrossRef\]](#)
- [22] Jianhua Z. Slight photo-electric signal test system. 2002;7:7–11.
- [23] Tabatabaee SA, Maroosi A. Deep learning-based receiver design for generalized frequency division multiplexing (GFDM). *Phys Commun* 2024;65:102390. [\[CrossRef\]](#)
- [24] Kordnoori S, Mostafeai H, Behzadi MH. Evaluation of the error performance of the IEEE802.16 standard based on a hidden Markov model. *Sigma J Eng Nat Sci* 2019;37:1480–1496.